

Effect of 3D printing technology-assisted TKA on cartilage tissue in rabbit with knee osteoarthritis

Guoliang Wang¹, Feng Cheng², Jianxun Cui², Nan Chen² and Qing Li²

¹Department of Sports Medicine, the First Affiliated Hospital of Kunming Medical University and ²Trauma Center of the First Affiliated Hospital of Kunming Medical University, Kunming City, Yunnan Province, PR China

Summary. Background. Knee osteoarthritis (KOA) is a common chronic degenerative joint disease. 3D printing technology has become one of the important directions of medical development along with individualized precision treatment in orthopedics.

Objective. To investigate the effect of 3D printing technology-assisted total knee arthroplasty (TKA) on cartilage in rabbits with KOA.

Methods. A rabbit model of KOA was established and treated by TKA or 3D printing-assisted TKA. Four weeks after treatment, radiological evaluation of rabbit knees was performed by X-ray examination, in order to observe the severity of osteoarthritic lesions. Then the knee joints of rabbits were collected for Hematoxylin-eosin, Toluidine blue, and Safranin O-Fast green staining. The expressions of cartilage matrix metabolism-related and apoptosis-related genes were scrutinized by real-time quantitative reverse transcription-polymerase chain reaction, Western blot, and immunohistochemistry. The levels of inflammatory-related factors in the cartilage tissues of rabbits were tested by enzyme-linked immunosorbent assay.

Results. In rabbits with KOA, 3D printing technology-assisted TKA alleviated the inflammation and bone remodeling of the knee joint, relieved synovial hyperplasia and inflammatory cell infiltration in the articular cartilage, reduced articular cartilage degradation, suppressed cartilage matrix metabolism, and mitigated the inflammatory response and apoptosis of cartilage cells.

Conclusion. 3D printing technology-assisted TKA exhibits a good treatment effect in rabbit KOA. This study provides an important basis for the clinical application of 3D printing technology-assisted TKA in KOA treatment.

Key words: Knee osteoarthritis, 3D printing-assisted TKA, Inflammation, Apoptosis, Articular cartilage degradation

Corresponding Author: Qing Li, 295 Xichang Road, Kunming City, Yunnan Province, 650032 PR China. e-mail: qing_li2021@163.com
www.hh.um.es. DOI: 10.14670/HH-18-743

Introduction

Knee osteoarthritis (KOA) is a common chronic degenerative joint disease, which is one of the major causes of disability. The global prevalence of KOA is about 22.9% in people over 40 years of age (Dainese et al., 2022). The pathogenesis of KOA involves multiple factors, such as articular cartilage destruction, ligament damage, synovial inflammation, bone osteophytes, etc. (Hunter and Bierma-Zeinstra, 2019). For patients with an early stage of KOA, physical and drug treatments are the preferred treatment strategies; however, for those with final stage KOA, surgical treatment is the recommended treatment strategy, which can greatly improve the life quality of patients (Geng et al., 2023).

Total knee arthroplasty (TKA), a new treatment technique for knee disorders, has shown significant benefits in improving knee function and relieving knee pain after successful TKA surgery; therefore, if all non-surgical treatments are ineffective, clinicians are encouraged to use TKA for patients with final stage KOA (Loures et al., 2019). The achievement of favorable clinical outcomes largely depends on proper implant alignment and adequate soft-tissue balancing; however, implant loosening due to difficulties in precise implant size is an important cause of treatment failure in TKA (Sheth et al., 2017). In recent years, 3D printing technology has developed rapidly in the medical field, mainly for *in vitro* medical models, human organs, and tissues, with the advantages of personalization, precision, remoteness, etc. (Inzana et al., 2014; Schubert et al., 2014; Fasel et al., 2016; Londhe et al., 2022). 3D printing technology-assisted TKA has been used in the clinical treatment of KOA accompanied by extra-articular deformity. It exhibits better clinical outcomes and patient satisfaction as it greatly improves the functional recovery of the knee joint and no adverse effects occur after surgery (Xu et al., 2017). 3D printing technology allows the creation of highly porous implants, which promotes osseointegration into the implants and then avoids aseptic loosening after TKA (Hasan et al., 2020). Furthermore, the application of 3D printing technology in TKA significantly reduces



operative time and postoperative bleeding (Liu et al., 2018). Currently, there is still insufficient data regarding the adjunctive use of 3D printing technology in TKA in the treatment of KOA. More data are still needed to support the widespread use of this technology in clinical settings.

In this study, a rabbit model of KOA was established and treated by 3D printing technology-assisted TKA, in order to investigate whether the aid of 3D printing technology can improve the effectiveness of TKA. This paper will provide more evidence for the clinical use of 3D printing technology to assist TKA in the clinical treatment of KOA.

Materials and methods

Animals and treatment

A total of 30 New Zealand White rabbits weighing 2.5 kg were commercially supplied by Jiagan Biotechnology (Shanghai, China). Rabbits were individually kept in a 12h day/night cycle room (free of specific pathogens) at 22°C. Food and water were freely available. Before surgery, rabbits were adaptively fed for one week. Animal experiments were implemented after being ratified by the Animal Ethics Committee of Kunming Medical University (kmmu20220372).

The animal experiment design followed the "3R principle" (Parker and Browne, 2014). The 30 rabbits were randomly divided into five groups: Control, KOA, Sham, TKA, and TKA+3D. There were six rabbits in each group. The treatment of rabbits in each group was as follows:

Control group: Rabbits did not undergo surgery. After three weeks of rearing, the rabbits were deeply anesthetized with 5% isoflurane. The radiological evaluation of the right posterior knees was performed by X-ray examination. Rabbits were then euthanized to collect the right posterior knee joints. These joints were kept at -80°C.

KOA group: Rabbits only underwent the construction of the model. The establishment of the KOA model was performed as previously reported (Li et al., 2016): rabbits underwent intra-articular injection of 4% papain (Solarbio, Beijing, China) (0.3 mL, diluted into saline) into the right posterior knee cavity on days 1, 4, and 7. After injection, rabbits were put back into their cages for three weeks of rearing. Three weeks later, the rabbits were deeply anesthetized with 5% isoflurane and then subjected to radiological evaluation and collection of the right posterior knee joints. The joints were kept at -80°C.

Sham group: Rabbits were first subjected to the construction of the KOA model. Three weeks later, the synovectomy was carried out as described previously (Riegels-Nielsen et al., 1991): rabbits were anesthetized with 2% isoflurane. The right posterior knees were debrided and the skin was disinfected. A medial parapatellar incision was then made and, after the knee

was opened, the synovial tissues were removed. Finally, the wound was closed with sutures. After the synovectomy, rabbits were kept for four weeks and moved freely. The rabbits were then deeply anesthetized with 5% isoflurane. Radiological evaluation and collection of the right posterior knee joints were performed.

TKA group: Rabbits first underwent the construction of the KOA model. Three weeks later, TKA was performed to treat these rabbits. The TKA procedure was conducted as follows: after being anesthetized with 2% isoflurane, the right posterior knees of these rabbits were debrided and the skin was disinfected. A longitudinal incision (3 cm in length) was made in the middle of the right posterior knee. The parapatellar tissue and joint capsule were incised longitudinally on the medial side of the patella to expose the joint cavity. After the patella was externalized, the knee joint was flexed and then the prosthesis was implanted. Finally, the wound was sutured. The right posterior knees of rabbits were immobilized for one week. One week later, these rabbits were allowed to move freely. Four weeks after TKA, these rabbits were deeply anesthetized with 5% isoflurane, followed by radiological evaluation and collection of the right posterior knee joints.

TKA + 3D group: Rabbits were first subjected to the construction of the KOA model. Three weeks later, 3D printing technology-assisted TKA was utilized to treat these rabbits. The procedure was as follows (Zhang et al., 2017; Jeong et al., 2021): The right posterior leg of each rabbit was scanned via magnetic resonance imaging using a 3.0-Tesla Signa HDx scanner (GE Healthcare, Milwaukee, WI, USA). The data from the magnetic resonance imaging was then imported into the Mimics software system (version 19.0, Materialize, Leuven, Belgium) in order to generate an accurate 3D reconstructed model. Then the 3D scaffold was constructed via 3D printing technology with polycaprolactone (Qiamu Analytical Technology, Shanghai, China). Thereafter, TKA was performed on these rabbits with the aid of 3D printing technology. After TKA, the right posterior knees of these rabbits were immobilized for one week. Four weeks after TKA, these rabbits were deeply anesthetized with 5% isoflurane. Radiological evaluation and collection of the right posterior knee joints were then performed.

Radiological evaluation

X-ray examination was performed on the knee joints of rabbits in each group, with the following parameters: 42 kV, 250 mA, 32 ms, and 80 cm film-focus distance. To evaluate the damage in the knee joints, the Kellgren-Lawrence (K-L) scale system was utilized with the previously reported scoring criteria (Liang et al., 2017).

Hematoxylin-eosin (HE) staining

The knee joints of rabbits in each group were fixed

KOA treatment by 3D printing-assisted TKA

in 4% paraformaldehyde for two days. After being decalcified with 10% ethylene diamine tetraacetate (EDTA) solution (Solarbio, Beijing, China) for 21 days, the knee joints were embedded into paraffin and cut into sections (5 μm in thickness). Afterward, the sections were treated with xylene and gradients of alcohol for dewaxing and rehydration. Hematoxylin solution (Solarbio, Beijing, China) and eosin solution (Solarbio, Beijing, China) were sequentially added to the sections for staining. The staining time for the hematoxylin solution was 5 min and 1 min for eosin. The residual staining solution was washed off with tap water. The sections were disclosed in neutral resin and observed under an optical microscope (BX51, Olympus, Tokyo, Japan), after being dehydrated with gradients of alcohol and xylene. The degree of osteoarthritis (OA) was evaluated by the Mankin scoring system.

Toluidine blue staining

The knee joints of rabbits from each group were immobilized in 4% paraformaldehyde for two days, decalcified with 10% EDTA for 21 days, embedded into paraffin, and then prepared into sections (5 μm in thickness). The dewaxing and rehydration of these sections were finished with xylene and alcohol gradient treatment. Then, 0.1% toluidine blue solution (Solarbio, Beijing, China) was added to the sections for 10 min staining at 25°C. The residual staining solution was washed away. These sections were then treated with gradients of alcohol and xylene for dehydration. After being sealed in neutral resin, the sections were placed under an optical microscope (BX51, Olympus, Tokyo, Japan) for observation. The International Cartilage Repair Society (ICRS) scoring system was utilized to assess the cartilage damage.

Safranin O-Fast green staining

The rabbit knee joints were immobilized in 4% paraformaldehyde for two days and then decalcified with 10% EDTA for 21 days. After paraffin-embedded, the joints were sectioned to a thickness of 5 μm . The

sections were dewaxed and rehydrated with xylene and gradients of alcohol. Fast green solution (Solarbio, Beijing, China) and Safranin O solution (Solarbio, Beijing, China) were sequentially utilized to stain the sections for 5 min at 25°C. After being dehydrated with anhydrous ethanol and xylene, the sections were sealed in neutral resin and observed under an optical microscope (BX51, Olympus, Tokyo, Japan). The Osteoarthritis Research Society International (OARSI) scoring system was utilized to assess the pathology of the rabbit knee joints.

Real-time quantitative reverse transcription-polymerase chain reaction (qRT-PCR)

Total RNA from the knee cartilage of rabbits from each group was extracted via a Total RNA Extraction Kit (Solarbio, Beijing, China) according to the directions. The reverse transcription reaction was then implemented for the synthesis of cDNA templates by applying a High-Capacity cDNA Reverse Transcription Kit (Applied Biosystems, Foster City, CA, USA). qRT-PCR was performed on a 7500 Real-Time PCR System (Applied Biosystems, Foster City, CA, USA) under the following conditions: 30 s at 95°C, and 40 cycles of 5 s at 95°C, 30 s at 55°C, and 30 s at 72°C. The relative mRNA expression of MMP-1, MMP-3, MMP-13, ADAMTS-5, Collagen II, Aggrecan, Bax, Bcl-2, and Caspase-3 was determined by the $2^{-\Delta\Delta C_t}$ method with normalizing to β -actin. The primers are shown in Table 1.

Enzyme-linked immunosorbent assay (ELISA)

The knee cartilage of rabbits from each group was collected and homogenized in lysis buffer (Beyotime, Shanghai, China) for 30 min on ice. The supernatant samples from each group were harvested by centrifugation (14,000 g and 4°C) for 15 min. The levels of TNF- α , IL-6, and IL-1 β were evaluated using commercial ELISA Kits (Solarbio, Beijing, China) in line with the directions. The absorbance value was read at 450 nm under a microplate reader (Molecular Devices, Sunnyvale, CA, USA).

Table 1. PCR primers.

Gene name	Forward (5' to 3')	Reverse (5' to 3')
MMP-1	TGTTTCAGTGGTGATGTTTCAGTTAGC	TATTTCTCCCCGAATTGTGGTTATAGC
MMP-3	AATGGACAAAGGATACAACAGGAACC	CATCATCTTGAGAAAGCGGAACC
MMP-13	TGAGATCATACTACCATCTCTGAATCC	CAAGTTTGCCTGTCACCTCTAAGC
ADAMTS-5	CTTCCACTAAGTAGTCCATGTAGATTGC	GGTCATTCCGATGTGGATTGC
Collagen II	AAGAGCGGTGACTACTGGAT	ACGCTGTTCTTGCAGTGGTA
Aggrecan	ATCTACCGCTGTGAGGTGAT	CTCCTGGAAGGTGAACCTTCT
Bax	CACCAAGAAGCTGAGCGAGT	GCAAAGTAAACAGGGCGACA
Bcl-2	GACGACTTCTCCCGCGCTA	ACACATGACCCACCGAAC
Caspase-3	AGATGTAAATGCAGCAAACCTC	TCCTTCATCACCGTGGCTT
β -actin	ATGTTTGTGATGGGCGTGAA	CGAAGTGGTCGTGGATGA

Western blot

The knee cartilage of rabbits was homogenized in radioimmunoprecipitation assay (RIPA) lysis buffer (Beyotime, Shanghai, China) on ice for 30 min to collect total protein. The homogenate was centrifuged for 15 min at 14,000 g and 4°C to collect the supernatant. The total protein concentration in the supernatant was scrutinized with a BCA Kit (Beyotime, Shanghai, China). A total of 30 µg of each supernatant sample was collected for 10% sodium dodecyl sulfate-polyacrylamide gel electrophoresis (SDS-PAGE). After being transferred to polyvinylidene fluoride (PVDF) membranes, the proteins were blocked for 1h in 5% skimmed milk. Afterwards, the proteins on the PVDF membranes were probed with primary antibodies (1:1000) for 12h at 4°C, and then horseradish peroxidase-conjugated goat anti-rabbit secondary antibody (1:2000; 4030-05, AmyJet Scientific, Wuhan, China) for 2h at 25°C. The development of specific protein blots was finished by treatment with enhanced chemiluminescence (ECL) reagent (Beyotime, Shanghai, China). Image J software (version 1.46r, ImageJ, NIH, Bethesda, MD, USA) was utilized to quantify the level of proteins by normalizing to β-actin protein. The information about the primary antibodies utilized in this research is shown in Table 2.

Immunohistochemistry

The knee joints of rats from each group were immobilized in 4% paraformaldehyde for two days before being paraffin-embedded. Then, the knee joints were sectioned to a thickness of 5 µm. The sections were dewaxed with xylene, rehydrated with gradients of alcohol, and subjected to the removal of endogenous peroxidase by 3% H₂O₂ treatment (10 min at 25°C) and antigen repair in boiling citric acid buffer for 10 min. Thereafter, 5% normal goat serum was utilized to block the sections for 30 min at 37°C. Rabbit anti-Bax (1:100; ab53154, Abcam, Shanghai, China), anti-Bcl-2 (1:100; ab59348, Abcam, Shanghai, China), and anti-Caspase-3 (1:100; ab184787, Abcam, Shanghai, China) were individually applied to treat the sections for 12h at 4°C.

After being reacted with horseradish peroxidase-conjugated goat anti-rabbit secondary antibody (1:200; 4030-05, AmyJet Scientific, Wuhan, China) for 30 min at 37°C, the sections were stained with 3,3'-diaminobenzidine (DAB) for 5 min at 25°C, and then counterstained with hematoxylin for 30 s at 25°C. The dehydration of the sections was implemented by treatment with gradients of alcohol and xylene. The neutral resin was utilized to disclose the sections, which were then observed under an optical microscope (BX51, Olympus, Tokyo, Japan). The expression of Bax, Bcl-2, and Caspase-3 proteins in cartilage tissues was evaluated by a semi-quantitative scoring system as previously reported (Deuster et al., 2019).

Statistical analysis

All experiments in this study were repeated three times independently to rule out chance in the results. All data were processed into the form of mean ± standard deviation. GraphPad Prism 6 (GraphPad Software, San Diego, CA, USA) was utilized for data analysis and production of statistical graphs. Data comparison among the five groups was assessed by one-way analysis of variance with post-hoc Tukey's test. *P*<0.05 indicated a statistically significant difference.

Results

3D printing technology-assisted TKA alleviated the inflammation and bone remodeling of the knee joint in KOA rabbits

The knee joints of rabbits were obtained. As shown in Figure 1A, rabbits from the Control group presented a glossy and uninterrupted cartilage surface. However, severe cartilage congestion, cartilage thickening, cartilage surface roughness, and a large amount of synovial fluid leakage were observed in rabbits from the KOA and Sham groups. Relative to the Sham group, KOA severity was obviously relieved in rabbits from the TKA and TKA + 3D groups. This remission effect was more pronounced in the TKA + 3D group.

Radiological evaluation was utilized to observe

Table 2. Primary antibodies for Western blot.

Primary antibody	Catalog number	Manufacturer
Rabbit anti-MMP-1	PAB11701	AmyJet Scientific (Wuhan, China)
Rabbit anti-MMP-3	PAB4795	AmyJet Scientific (Wuhan, China)
Rabbit anti-MMP-13	D120098	Sangon Biotech (Shanghai, China)
Rabbit anti-ADAMTS-5	PAB25974	AmyJet Scientific (Wuhan, China)
Rabbit anti-Collagen II	70R-CR008	AmyJet Scientific (Wuhan, China)
Rabbit anti-Aggregan	MBS822299	AmyJet Scientific (Wuhan, China)
Rabbit anti-TNF-α	ABP52624	AmyJet Scientific (Wuhan, China)
Rabbit anti-IL-6	PAB27749	AmyJet Scientific (Wuhan, China)
Rabbit anti-IL-1β	ABP52932	AmyJet Scientific (Wuhan, China)
Rabbit anti-β-actin	ABP50590	AmyJet Scientific (Wuhan, China)

KOA treatment by 3D printing-assisted TKA

changes in the rabbit knee joint. The X-ray is displayed in Figure 1B. Radiological signs of severe osteoarthritis, mild joint space narrowing, and osteophyte formation were observed in rabbits from the KOA and Sham groups. These phenomena were alleviated in the rabbit knee joints from the TKA and TKA + 3D groups. The alleviation was more obvious in rabbits of the TKA + 3D group. The K-L system was utilized to evaluate the X-ray results (Fig. 1C). A higher K-L score was obtained in rabbits from the KOA and Sham groups, compared with the Control group ($P<0.001$). Conversely, rabbits from the TKA and TKA + 3D groups had lower K-L scores than the Sham group ($P<0.01$). Simultaneously, when matched to the TKA group, the K-L score was much lower in rabbits from the TKA + 3D group ($P<0.01$). All of these results implied that 3D printing technology-assisted TKA could relieve the inflammation and bone remodeling of the knee joint in KOA rabbits.

3D printing technology-assisted TKA reduced articular cartilage degradation in KOA rabbits

HE staining of rabbit articular cartilage exhibited that, rabbits from the Control group presented normal cell distribution and synovium thickness. However, obvious synovial hyperplasia as well as inflammatory cell infiltration was observed in the synovium of rabbits from the KOA and Sham groups. When compared with

the Sham group, inflammatory cell infiltration and synovial hyperplasia were relieved in rabbits from the TKA and TKA + 3D groups. Meanwhile, these signs were further mitigated in rabbits from the TKA + 3D group compared with the TKA group. The cartilage of rabbits was evaluated with the Mankin score. The highest Mankin scores were found in rabbits from the KOA and Sham groups when matched against the Control group ($P<0.001$). However, it was much decreased in the TKA and TKA + 3D groups, compared with the Sham group ($P<0.01$). Intriguingly, rabbits from the TKA + 3D group had lower Mankin scores than the TKA group ($P<0.01$) (Fig. 2A).

Toluidine blue staining of rabbit articular cartilage was implemented. The homogenous deep blue staining of the articular cartilage matrix was observed in rabbits from the Control group. However, the thin articular cartilage and the irregular articular surface occurred in rabbits from the TKA and TKA + 3D groups. Interestingly, the blue staining of the articular cartilage matrix was enhanced and the irregular articular surface was relieved in rabbits from the TKA + 3D group when matched against the TKA group. The ICRS score for toluidine blue staining was higher in rabbits from the KOA and Sham groups than in the Control group ($P<0.001$). Contrastingly, the much-decreased ICRS score was in rabbits from the TKA and TKA + 3D groups, relative to the Sham group ($P<0.01$).

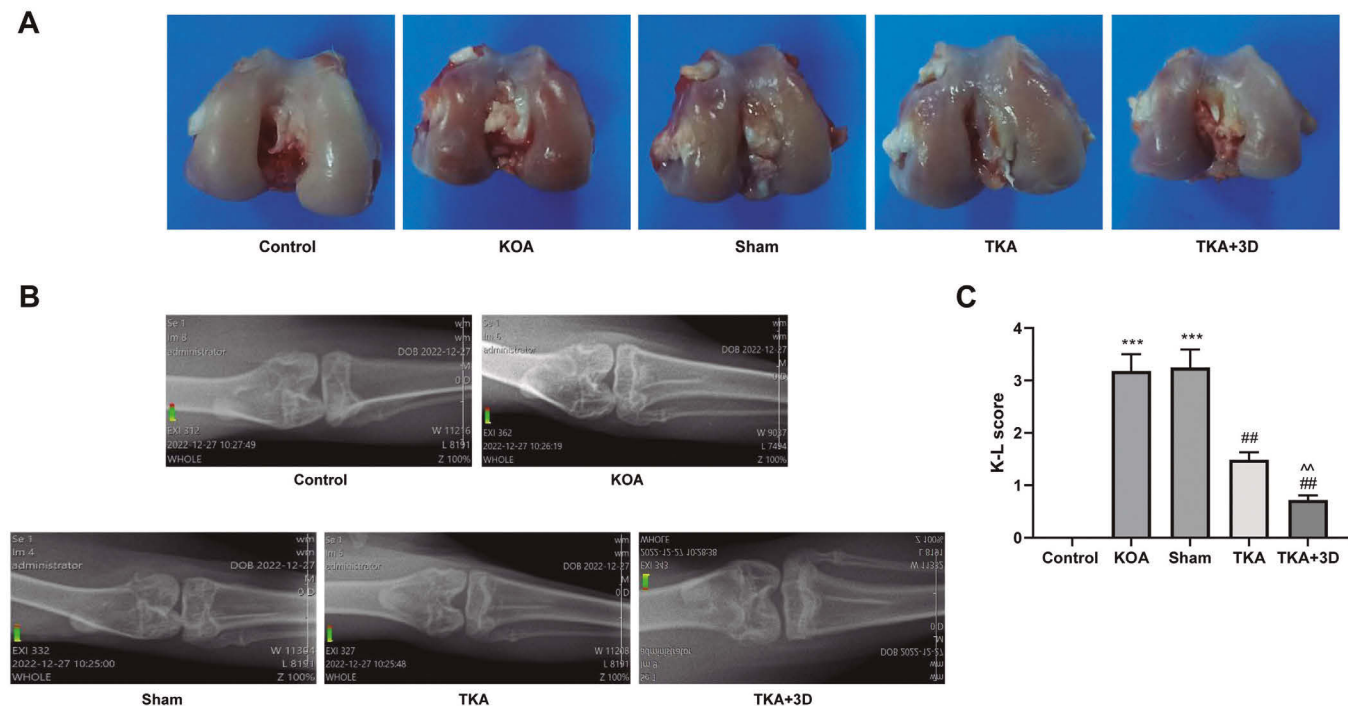


Fig. 1. 3D printing technology-assisted TKA treatment alleviated inflammation and bone remodeling of the knee joint in KOA rabbits. **A.** 3D printing technology-assisted TKA relieved articular cartilage damage in rabbits induced by KOA. $n=6$. **B, C.** X-ray was performed on rabbits, and the K-L system was utilized to evaluate the X-ray results. 3D printing technology-assisted TKA treatment relieved the severity of KOA in rabbits. $n=6$. *** $P<0.001$ vs. the Control group. ## $P<0.01$ vs. the Sham group. ^^ $P<0.01$ vs. the TKA group.

KOA treatment by 3D printing-assisted TKA

Additionally, rabbits from the TKA + 3D group had a much lower ICRS score than the TKA group ($P<0.01$) (Fig. 2B).

Safranin O-Fast green staining showed normal cellularity, integrated surface, and consistent matrix staining in rabbits from the Control group. However, severe joint wear and cartilage matrix loss were found in rabbits from the KOA and Sham groups. Compared with the Sham group, the joint wear and cartilage matrix loss were much mitigated in rabbits from the TKA and TKA + 3D groups. At the same time, joint wear and cartilage matrix loss were still present in rabbits from the TKA + 3D group, however, the severity was much milder than in the TKA group. Furthermore, a much higher OARSI score was obtained in rabbits from the KOA and Sham groups, when matched against the Control group ($P<0.001$). However, the OARSI score was significantly decreased in rabbits from the TKA and TKA + 3D groups, in contrast to the Sham group ($P<0.01$). Rabbits from the TKA + 3D group had a lower OARSI score than the TKA group ($P<0.01$) (Fig. 2C). Therefore, 3D printing technology-assisted TKA attenuated articular cartilage degradation in KOA rabbits.

3D printing technology-assisted TKA suppressed the metabolism of cartilage matrix in KOA rabbits

The mRNA expression of MMP-1, MMP-3, MMP-13, ADAMTS-5, Collagen II, and Aggrecan in the knee

cartilage of rabbits was scrutinized via qRT-PCR. As presented in Figure 3A,B, the elevated mRNA expression of MMP-1, MMP-3, MMP-13, and ADAMTS-5, as well as the reduced mRNA expression of Collagen II and Aggrecan, were observed in rabbit knee cartilage from the KOA and Sham groups, compared with the Control group ($P<0.001$). An opposite result was seen in rabbit knee cartilage from the TKA and TKA + 3D groups, compared with the Sham group ($P<0.05$, $P<0.01$, and $P<0.001$). Matched with the TKA group, the knee cartilage of rabbits from the TKA + 3D group exhibited much lower mRNA expression of MMP-1, MMP-3, MMP-13, ADAMTS-5, as well as higher mRNA expression of Collagen II and Aggrecan ($P<0.05$). By Western blot, similar results were discovered for the expression of MMP-1, MMP-3, MMP-13, ADAMTS-5, Collagen II, and Aggrecan proteins in the knee cartilage of rabbits from each group (Fig. 3C). Thus, treatment with 3D printing technology-assisted TKA prevented the metabolism of cartilage matrix in KOA rabbits.

3D printing technology-assisted TKA relieved the inflammatory response in KOA rabbits

To evaluate the inflammatory response in KOA rabbits, this study used ELISA and Western blot to detect the expression of TNF- α , IL-6, and IL-1 β in knee cartilage. The data are shown in Figures 4A,B. In

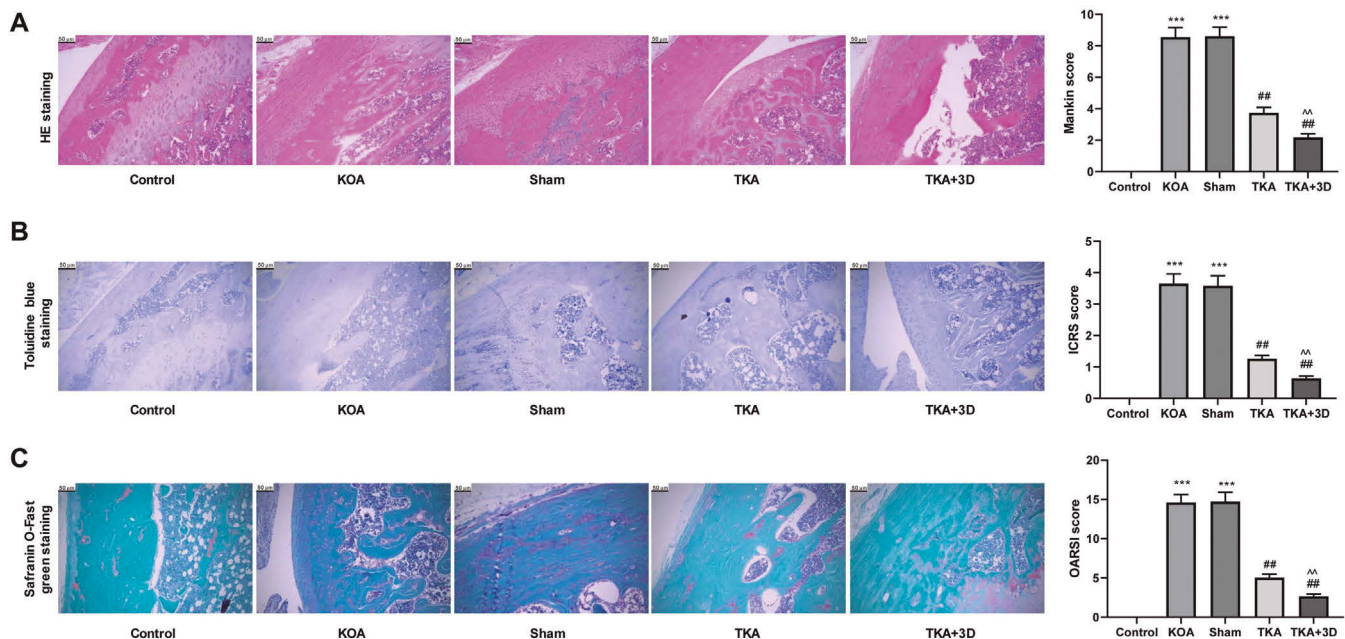


Fig. 2. 3D printing technology-assisted TKA treatment reduced articular cartilage degradation in KOA rabbits. **A.** HE staining and Mankin score suggested that treatment with 3D printing technology-assisted TKA attenuated inflammatory cell infiltration and synovial hyperplasia in KOA rabbits. $n=6$. **B.** Toluidine blue staining and ICRS score indicated that 3D printing technology-assisted TKA treatment increased articular cartilage matrix staining and relieved the irregular articular surface in KOA rabbits. $n=6$. **C.** Safranin O-Fast green staining and OARSI score revealed that treatment with 3D printing technology-assisted TKA relieved joint wear and cartilage matrix loss. $n=6$. *** $P<0.001$ vs. the Control group. ## $P<0.01$ vs. the Sham group. ^^ $P<0.01$ vs. the TKA group. $\times 200$.

KOA treatment by 3D printing-assisted TKA

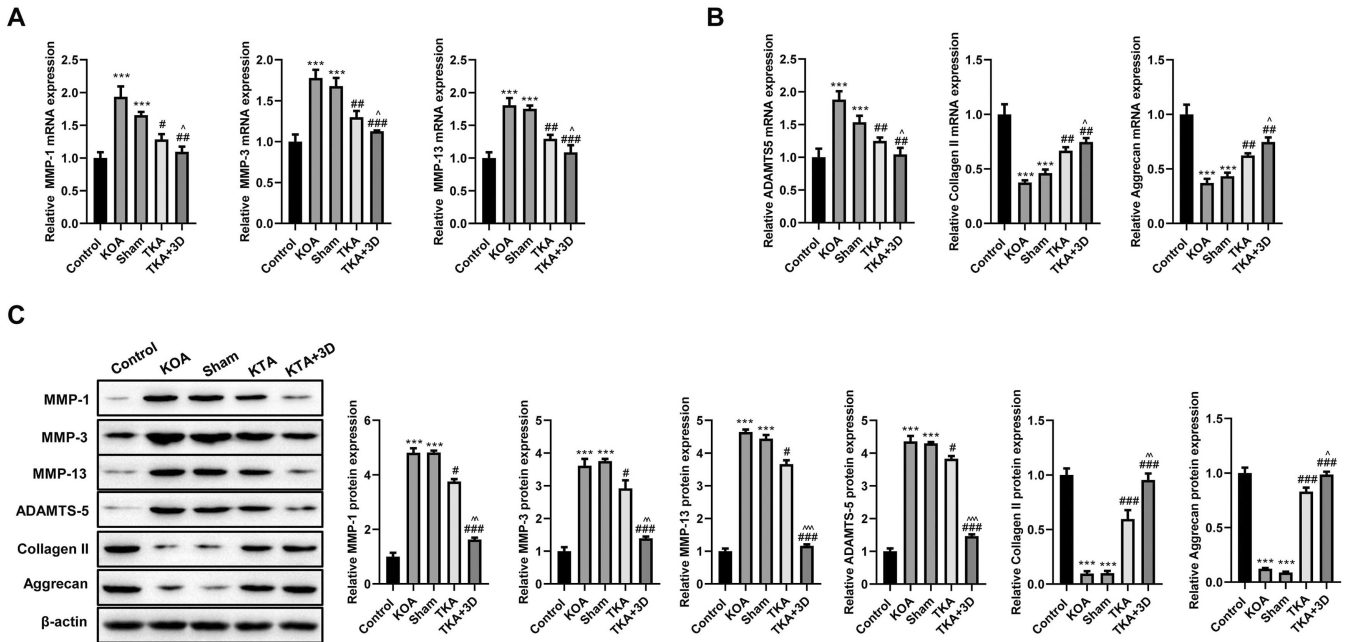


Fig. 3. 3D printing technology-assisted TKA treatment suppressed cartilage matrix metabolism in KOA rabbits. **A-C.** qRT-PCR and Western blot were performed to study the expression of metabolism-related genes in the knee cartilage of rabbits. It was revealed that treatment with 3D printing technology-assisted TKA prevented cartilage matrix metabolism in KOA rabbits by regulating the expression of these metabolism-related genes. n=6. *** $P < 0.001$ vs. the Control group. # $P < 0.05$, ## $P < 0.01$ and ### $P < 0.001$ vs. the Sham group. ^ $P < 0.05$, ^^ $P < 0.01$ and ^^ $P < 0.001$ vs. the TKA group.

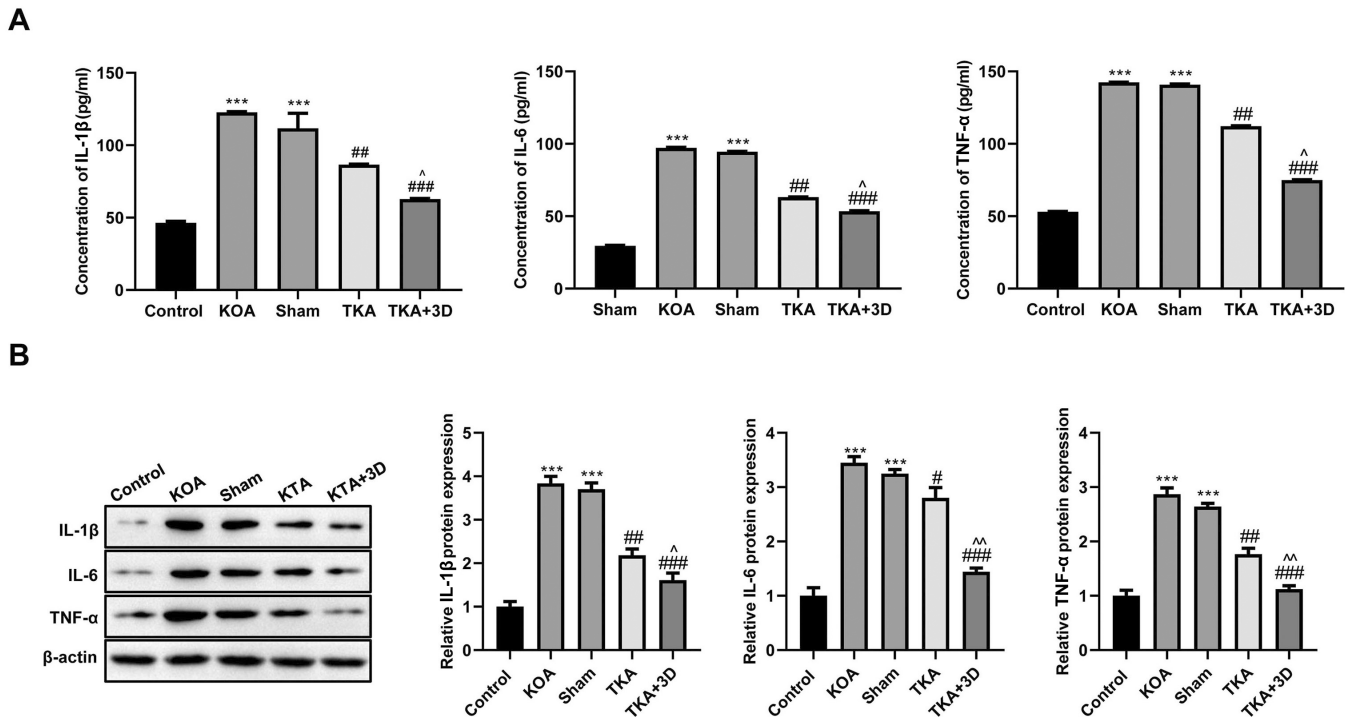


Fig. 4. 3D printing technology-assisted TKA treatment relieved the inflammatory response in KOA rabbits. **A, B.** ELISA and Western blot were implemented to detect the inflammatory response in rabbit knee cartilage via detecting the expression of pro-inflammatory genes. 3D printing technology-assisted TKA suppressed the inflammatory response in KOA rabbits as it reduced the expression of TNF- α , IL-6, and IL-1 β in knee cartilage. n=6. *** $P < 0.001$ vs. the Control group. # $P < 0.05$, ## $P < 0.01$ and ### $P < 0.001$ vs. the Sham group. ^ $P < 0.05$ and ^^ $P < 0.01$ vs. the TKA group.

KOA treatment by 3D printing-assisted TKA

comparison with the Control group, rabbits from the KOA and Sham groups showed higher expression of TNF- α , IL-6, and IL-1 β proteins in the knee cartilage ($P<0.001$). Relative to the Sham group, the expression of TNF- α , IL-6, and IL-1 β proteins were all decreased in rabbit knee cartilage from the TKA and TKA + 3D groups ($P<0.05$, $P<0.01$, and $P<0.001$). Furthermore, rabbits from the TKA + 3D group had a lower expression of TNF- α , IL-6, and IL-1 β proteins in their knee cartilage than the TKA group ($P<0.05$ and $P<0.01$). Hence, treatment with 3D printing technology-assisted TKA mitigated the inflammatory response in KOA rabbits.

3D printing technology-assisted TKA attenuated apoptosis in KOA rabbits

This study detected the mRNA and protein expression of Bax, Bcl-2, and Caspase-3 in rabbit knee cartilage by qRT-PCR and immunohistochemistry (IHC), in order to evaluate the apoptosis of knee chondrocytes. We found higher Bax and Caspase-3 but lower Bcl-2 expression in rabbit knee cartilage from the KOA and Sham groups than the Control group ($P<0.01$ and $P<0.001$). However, when contrasted with the Sham group, rabbits from the TKA and TKA + 3D groups expressed lower Bax and Caspase-3 but higher Bcl-2 in

knee cartilage ($P<0.05$, $P<0.01$, and $P<0.001$). Also, lower Bax and Caspase-3 but higher Bcl-2 expression occurred in rabbit knee cartilage from the TKA + 3D group in comparison with the TKA group ($P<0.05$ and $P<0.01$) (Fig. 5A-C). These data illustrate that treatment with 3D printing technology-assisted TKA relieved the apoptosis of knee chondrocytes in KOA rabbits.

Discussion

3D printing technology is predicted to potentially change regenerative medicine in a fundamental way as it will enable organs and tissues to be printed on demand (Nguyen et al., 2017). It has been reported that, compared with conventional TKA, 3D printing technology-assisted TKA allows for a personalized preoperative plan and avoids multiple osteotomies due to visual errors, loosening of the prosthesis, and infection caused by the opening of the medullary cavity (Xu et al., 2017). The present work focused on the effect of 3D printing technology-assisted TKA in the treatment of KOA in rabbit models. It was suggested that 3D printing technology-assisted TKA was more effective in treating KOA than traditional TKA. As we know, cartilage lesions, such as cartilage congestion, thickening, and surface roughness, represent the main features of OA (Loeuille et al., 2009; Newton et al., 2017; Totlis et al.,

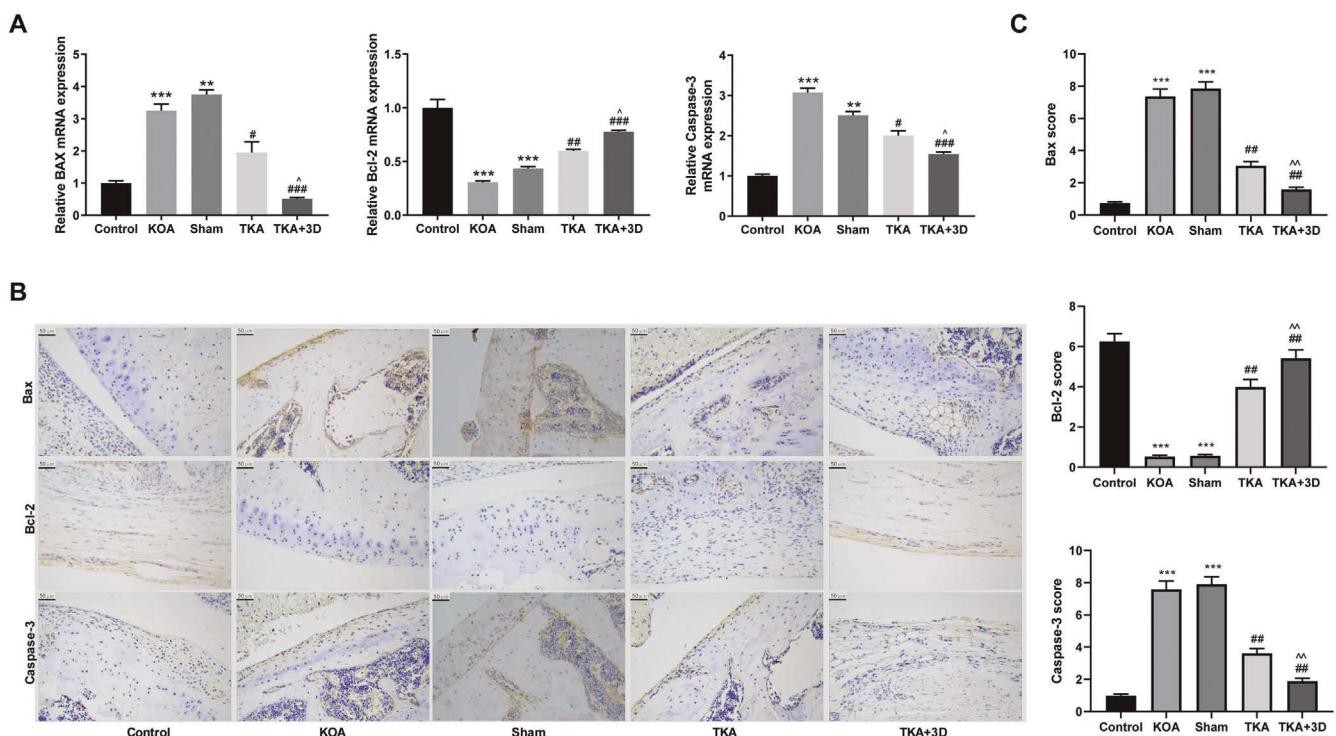


Fig. 5. 3D printing technology-assisted TKA treatment relieved the apoptosis of knee chondrocytes in KOA rabbits. **A-C.** By qRT-PCR and IHC, 3D printing technology-assisted TKA treatment relieved the apoptosis of knee chondrocytes in KOA rabbits as it reduced the expression of Bax and Caspase-3 but elevated the expression of Bcl-2 in the knee cartilage of KOA rabbits. $n=6$. ** $P<0.01$ and *** $P<0.001$ vs. the Control group. # $P<0.05$, ## $P<0.01$ and ### $P<0.001$ vs. the Sham group. ^ $P<0.05$ and ^^ $P<0.01$ vs. the TKA group. $\times 200$.

2021; Liu et al., 2022). In addition, osteophyte formation is another key radiographic sign of OA and restricted motion in KOA (Wu et al., 2023). Meanwhile, excessive synovial fluid leakage can accelerate the degeneration of joint tissues and eventually leads to limited movement (Olesiak and Przedborska, 2022). This study implied that 3D printing technology-assisted TKA can mitigate these pathological features of KOA more significantly than traditional TKA. Traditional TKA mainly relies on the surgeon's experience to determine the anatomical position and the amount of bone grafting, which carries various problems, such as limited osteotomy accuracy, multiple osteotomies during surgery, longer operation time, severe surgical trauma, increased blood loss, and infection risk. A 3D-printed scaffold has high precision and consistency as it can achieve individual customization and precise osteotomy; moreover, 3D printing technology can greatly reduce prosthesis implantation error and surgical trauma, shorten the operation time, and reduce the risk of infection (Liu et al., 2018). Polycaprolactone is a commonly used medical scaffold material for bone engineering, possessing multiple advantages such as biocompatibility, proper mechanical strength, and low cost (Abpeikar et al., 2021). Thus, polycaprolactone was employed in this study.

Additionally, this study performed histological staining on the knee joint of KOA rabbits in order to microscopically observe cartilage changes. It was revealed that 3D printing technology-assisted TKA relieved cartilage matrix degradation in KOA rabbits. The destruction of articular cartilage is a major feature of KOA and it is induced by the homeostatic imbalance between synthesis and degradation of extracellular matrix components (Li and Wu, 2021). Currently, the products of cartilage matrix degradation are proposed as biomarkers for OA diagnosis, such as matrix metalloproteinases (MMPs), which are primarily responsible for the degradation of the extracellular matrix. Chondrocytes are capable of producing MMP-3 and then degrading the main component of articular cartilage (such as Collagen II) by activating MMP-1 and MMP-13 (Oğuz et al., 2021). Collagen II and Aggrecan are essential components of articular cartilage, whereas ADAMTS-5 is another crucial enzyme responsible for the degradation of collagen (Thompson et al., 2015; Higuchi et al., 2017; Zhang et al., 2022). In this research, 3D printing technology-assisted TKA was more effective in preventing the degradation of cartilage matrix in KOA rabbits as it greatly suppressed the expression of the MMP-1, MMP-3, MMP-13, and ADAMTS-5 proteins, and increased the expression of Collagen II and Aggrecan proteins, more than traditional TKA.

Inflammation is an important pathological feature of KOA, and its role in the progression of KOA has become a research hotspot (Ioan-Facsinay and Kloppenburg, 2013). The HE staining in this work suggested severe inflammatory cell infiltration in the articular cartilage of KOA rabbits. Meanwhile, the

increased expression of TNF- α , IL-6, and IL-1 β was observed in cartilage tissues of KOA rabbits. TNF- α , IL-6, and IL-1 β are the main pro-inflammatory factors in KOA, which can be produced by chondrocytes and then exacerbate KOA development by driving the inflammatory cascade response and destroying chondrocytes (Shi et al., 2020; Rai et al., 2022). Interestingly, 3D printing technology-assisted TKA distinctly reduced the inflammatory response as it reduced the expression of TNF- α , IL-6, and IL-1 β in articular cartilage tissues of KOA rabbits. As previously reported, 3D printing technology-assisted TKA ensures precise osteotomy and reduces surgical trauma and infection risk compared with traditional TKA (Liu et al., 2018). In this study, rabbits treated with 3D printing technology-assisted TKA showed lower levels of TNF- α , IL-6, and IL-1 β in articular cartilage tissues than those treated with traditional TKA. It could be that 3D printing technology-assisted TKA reduced surgical trauma and infections, which in turn led to the reduction in the expression of TNF- α , IL-6, and IL-1 β .

It has been reported that the apoptosis of chondrocytes is involved in OA pathogenesis; as the only cells in articular cartilage, the decreased survival of chondrocytes would lead to the degeneration and destruction of articular cartilage tissues, which is a predisposing factor for OA progression (Sun et al., 2021). This study detected upregulated Bax and Caspase-3 but downregulated Bcl-2 in the articular cartilage tissues of KOA rabbits. Intriguingly, 3D printing technology-assisted TKA was more effective in reducing Bax and Caspase-3 expression and inducing Bcl-2 expression than traditional TKA. Bax and Caspase-3 are apoptosis-promoting factors, and Bcl-2 exerts an anti-apoptotic effect in KOA; the three protein types can regulate the apoptosis of chondrocytes, ultimately resulting in cartilage degeneration (He et al., 2020). Thus, in this study, 3D printing technology-assisted TKA was more conducive to mitigating the apoptosis of chondrocytes in KOA than traditional TKA.

Conclusion

This study compared the effectiveness of 3D printing technology-assisted TKA and traditional TKA in treating rabbits with KOA. The results suggested that, in comparison with traditional TKA, 3D printing technology-assisted TKA produced better results for treating KOA. It was more capable of mitigating cartilage lesions, cartilage matrix degradation, inflammation, and apoptosis in chondrocytes after surgery. Therefore, we propose that 3D printing technology-assisted TKA will be widely utilized in the clinical practice of KOA treatment.

Conflict of interest. All authors declare that they have no competing interests.

Author's contributions. Contributions: (I) Conception and design: Qing Li; (II) Administrative support: Feng Cheng; (III) Provision of study

materials or patients: Jianxun Cui and Nan Chen; (IV) Collection and assembly of data: Wangguo Liang; (V) Data analysis and interpretation: Wangguo Liang; (VI) Manuscript writing: Wangguo Liang; (VII) Final approval of manuscript: All authors.

Ethical standards. Animal experiments were implemented after being ratified by the Animal Ethics Committee of Kunming Medical University (kmmu20220372).

Informed consent. n/a

Funding. This work was supported by the Yunnan Province Clinical Center for Bone and Joint Diseases (ZX2019-03-04)

Data availability statement. The datasets generated during and/or analyzed in the current study are available from the corresponding author upon reasonable request.

References

- Abpeikar Z., Moradi L., Javdani M., Kargozar S., Soleimannejad M., Hasanzadeh E., Mirzaei S.A. and Asadpour S. (2021). Characterization of macroporous Polycaprolactone/Silk fibroin/Gelatin/Ascorbic acid composite scaffolds and *in vivo* results in a rabbit model for meniscus cartilage repair. *Cartilage* 13, 1583s-1601s.
- Dainese P., Wyngaert K.V., De Mits S., Wittoek R., Van Ginckel A. and Calders P. (2022). Association between knee inflammation and knee pain in patients with knee osteoarthritis: A systematic review. *Osteoarthritis Cartilage* 30, 516-534.
- Deuster E., Mayr D., Hester A., Kolben T., Zeder-Göb C., Burges A., Mahner S., Jeschke U., Trillsch F. and Czogalla B. (2019). Correlation of the Aryl hydrocarbon receptor with FSHR in ovarian cancer patients. *Int. J. Mol. Sci.* 20, 2862.
- Fasel J.H., Aguiar D., Kiss-Bodolay D., Montet X., Kalangos A., Stimec B.V. and Ratib O. (2016). Adapting anatomy teaching to surgical trends: A combination of classical dissection, medical imaging, and 3D-printing technologies. *Surg. Radiol. Anat.* 38, 361-367.
- Geng R., Li J., Yu C., Zhang C., Chen F., Chen J., Ni H., Wang J., Kang K., Wei Z., Xu Y. and Jin T. (2023). Knee osteoarthritis: Current status and research progress in treatment (review). *Exp. Ther. Med.* 26, 481.
- Hasan S., van Hamersveld K.T., Marang-van de Mheen P.J., Kaptein B.L., Nelissen R. and Toksvig-Larsen S. (2020). Migration of a novel 3D-printed cementless *versus* a cemented total knee arthroplasty: Two-year results of a randomized controlled trial using radiostereometric analysis. *Bone Joint J.* 102-B, 1016-1024.
- He X., Wang L., Zhou X., Xu L., Cao J., Wang R., Wang M. and Xie G. (2020). Effect of Gubi prescription on caveolin-1 expression and phosphoinositide 3 kinase/protein kinase B and fas signal pathways in rats with knee osteoarthritis. *J. Tradit. Chin. Med.* 40, 224-235.
- Higuchi Y., Nishida Y., Kozawa E., Zhuo L., Arai E., Hamada S., Morita D., Ikuta K., Kimata K., Ushida T. and Ishiguro N. (2017). Conditional knockdown of hyaluronidase 2 in articular cartilage stimulates osteoarthritic progression in a mice model. *Sci. Rep.* 7, 7028.
- Hunter D.J. and Bierma-Zeinstra S. (2019). Osteoarthritis. *Lancet* 393, 1745-1759.
- Inzana J.A., Olvera D., Fuller S.M., Kelly J.P., Graeve O.A., Schwarz E.M., Kates S.L. and Awad H.A. (2014). 3D printing of composite calcium phosphate and collagen scaffolds for bone regeneration. *Biomaterials* 35, 4026-4034.
- Ioan-Facsinay A. and Kloppenburg M. (2013). An emerging player in knee osteoarthritis: The infrapatellar fat pad. *Arthritis Res. Ther.* 15, 225.
- Jeong H.J., Lee S.W., Hong M.W., Kim Y.Y., Seo K.D., Cho Y.S. and Lee S.J. (2021). Total meniscus reconstruction using a polymeric hybrid-scaffold: Combined with 3d-printed biomimetic framework and micro-particle. *Polymers* 13, 1910.
- Li S.H. and Wu Q.F. (2021). MicroRNAs target on cartilage extracellular matrix degradation of knee osteoarthritis. *Pharmacol. Sci.* 25, 1185-1197.
- Li F., Yin Z., Wu H., Qin Z., Li Z. and Qiu Y. (2016). Section of the anterior cruciate ligament in the rabbit as animal model for osteoarthritis progression. *Int. Orthop.* 40, 407-416.
- Liang Z., Wang X., Xu X., Xie B., Ji A., Meng S., Li S., Zhu Y., Wu J., Hu Z., Lin Y., Zheng X., Xie L. and Liu B. (2017). MicroRNA-608 inhibits proliferation of bladder cancer via AKT/FOXO3a signaling pathway. *Mol. Cancer* 16, 96.
- Liu D., Li Y., Cai G., Jia D., Mao J., Meng X., Wang G. and He C. (2018). Short-term effectiveness of total knee arthroplasty assisted by three-dimensional printing osteotomy navigation template. *Zhongguo. Xiu. Fu. Chong. Jian. Wai. Ke. Za. Zhi.* 32, 899-905 (in Chinese).
- Liu X., Pitner M.A., Baki P.P., Lu Q., Schroepfel J.P. and Wang J. (2022). Software-assisted quantitative measurement of osteoarthritic subchondral bone thickness. *J. Vis. Exp.* 18, 181.
- Loeuille D., Rat A.C., Goebel J.C., Champigneulle J., Blum A., Netter P., Gillet P. and Chary-Valckenaere I. (2009). Magnetic resonance imaging in osteoarthritis: Which method best reflects synovial membrane inflammation? Correlations with clinical, macroscopic and microscopic features. *Osteoarthritis Cartilage* 17, 1186-1192.
- Londhe S., Shetty S., Vora N., Shah A., Nair R., Shetty V., Desouza C. and Khan F. (2022). Efficacy of the pre-operative three-dimensional (3D) CT scan templating in predicting accurate implant size and alignment in robot assisted total knee arthroplasty. *Indian J. Orthop.* 56, 2093-2100.
- Loures F.B., Correia W., Reis J.H., Pires E.A.R.S., de Paula Mozela A., de Souza E.B., Maia P.V. and Barretto J.M. (2019). Outcomes after knee arthroplasty in extra-articular deformity. *Int. Orthop.* 43, 2065-2070.
- Newton M.D., Osborne J., Gawronski K., Baker K.C. and Maerz T. (2017). Articular cartilage surface roughness as an imaging-based morphological indicator of osteoarthritis: A preliminary investigation of osteoarthritis initiative subjects. *J. Orthop. Res.* 35, 2755-2764.
- Nguyen D., Hägg D.A., Forsman A., Ekholm J., Nimkingratana P., Brantsing C., Kalogeropoulos T., Zaunz S., Concaro S., Brittberg M., Lindahl A., Gatenholm P., Enejder A. and Simonsson S. (2017). Cartilage tissue engineering by the 3D bioprinting of iPS cells in a nanocellulose/alginate bioink. *Sci. Rep.* 7, 658.
- Oğuz R., Belviranlı M. and Okudan N. (2021). Effects of exercise training alone and in combination with kinesio taping on pain, functionality, and biomarkers related to the cartilage metabolism in knee osteoarthritis. *Cartilage* 13, 1791S-1800S.
- Olesiak B. and Przedborska A. (2022). Evaluation of the effect of excess synovial fluid on knee joint pain in patients with osteoarthritis. *Ortop. Traumatol. Rehabil.* 24, 325-333.
- Parker R.M. and Browne W.J. (2014). The place of experimental design and statistics in the 3Rs. *ILAR J.* 55, 477-485.
- Rai V., Dilisio M.F., Samadi F. and Agrawal D.K. (2022). Counteractive effects of IL-33 and IL-37 on inflammation in osteoarthritis. *Int. J.*

KOA treatment by 3D printing-assisted TKA

- Environ. Res. Public. Health. 19, 5690.
- Riegels-Nielsen P., Frimodt-Møller N., Sørensen M. and Jensen J.S. (1991). Synovectomy for septic arthritis. Early *versus* late synovectomy studied in the rabbit knee. Acta. Orthop. 62, 315-318.
- Schubert C., van Langeveld M.C. and Donoso L.A. (2014). Innovations in 3D printing: A 3D overview from optics to organs. Br. J. Ophthalmol. 98, 159-161.
- Sheth N.P., Husain A. and Nelson C.L. (2017). Surgical techniques for total knee arthroplasty: Measured resection, gap balancing, and hybrid. J. Am. Acad. Orthop. Surg. 25, 499-508.
- Shi G.X., Tu J.F., Wang T.Q., Yang J.W., Wang L.Q., Lin L.L., Wang Y., Li Y.T. and Liu C.Z. (2020). Effect of electro-acupuncture (EA) and manual acupuncture (MA) on markers of inflammation in knee osteoarthritis. J. Pain Res. 13, 2171-2179.
- Sun Y., Leng P., Guo P., Gao H., Liu Y., Li C., Li Z. and Zhang H. (2021). G protein coupled estrogen receptor attenuates mechanical stress-mediated apoptosis of chondrocyte in osteoarthritis via suppression of Piezo1. Mol. Med. 27, 96.
- Thompson C.L., Patel R., Kelly T.A., Wann A.K., Hung C.T., Chapple J.P. and Knight M.M. (2015). Hedgehog signalling does not stimulate cartilage catabolism and is inhibited by interleukin-1 β . Arthritis Res. Ther. 17, 373.
- Totlis T., Marín Fermín T., Kalifis G., Terzidis I., Maffulli N. and Papakostas E. (2021). Arthroscopic debridement for focal articular cartilage lesions of the knee: A systematic review. Surgeon 19, 356-364.
- Wu K.T., Wang Y.W., Wu R.W., Huang C.C. and Chen Y.C. (2023). Association of a femoral neck T score with knee joint osteophyte formation but not with skeletal muscle mass. Clin. Rheumatol. 42, 917-922.
- Xu Z., Wang W., Zhuang Z. and Zhang Y. (2017). Effectiveness of total knee arthroplasty using three-dimensional printing technology for knee osteoarthritis accompanied with extra-articular deformity. Zhongguo. Xiu. Fu. Chong. Jian. Wai. Ke. Za. Zhi. 31, 913-917 (in Chinese).
- Zhang Z.Z., Wang S.J., Zhang J.Y., Jiang W.B., Huang A.B., Qi Y.S., Ding J.X., Chen X.S., Jiang D. and Yu J.K. (2017). 3D-printed poly(ϵ -caprolactone) scaffold augmented with mesenchymal stem cells for total meniscal substitution: A 12- and 24-week animal study in a rabbit model. Am. J. Sports. Med. 45, 1497-1511.
- Zhang Y., Dai J., Yan L., Lin Q., Miao H., Wang X., Wang J. and Sun Y. (2022). DL-3-N-butylphthalide promotes cartilage extracellular matrix synthesis and inhibits osteoarthritis development by regulating FoxO3a. Oxid. Med. Cell. Longev. 2022, 9468040.

Accepted April 5, 2024